PHYSICAL REVIEW B VOLUME 27, NUMBER 7 1 APRIL 1983

Microscopic determination of the self-energy of ^{3}He

E. Krotscheck*
Department of Physics, University of Illinois at Urbana-Champaign, Urbana, Illinois 61801

R. A. Smith
Department of Physics, Texas A&M University, College Station, Texas 77843
(Received 7 May 1982)

From Planck's constant, the mass of a ^{3}He atom, and the "Hartree-Fock dispersion 2" potential (which describes ^{4}He quite well) we calculate the ground-state energy and the complex self-energy of liquid ^{3}He. The calculations are performed within the framework of correlated-basis-function theory. The starting point in this method is an optimized Fermi hypernetted-chain calculation. Improvements on the wave function are incorporated through nonorthogonal perturbation theory. For the energy, we include corrections of second and third order in the effective two-body interaction as well as second-order terms in the effective three-body interaction. Second- and third-order perturbative corrections to the self-energy of a ^{3}He atom reveal a rapid variation with both energy and momentum in the vicinity of the Fermi surface. This effect is shown to be due to the attractiveness of the effective interaction in the spin channel. Our results are in quantitative agreement with phenomenological determinations of the self-energy based on the experimental specific heat.

I. INTRODUCTION

The rapid variation of the specific heat of liquid ^{3}He at low temperatures[1] and the related question of the effective mass[2–4] is currently a subject of intensive theoretical study.[5,6] The paramagnon picture[5] is a qualitative description of the effect; under certain assumptions semimicroscopic arguments[6] allow the self-energy and hence the energy-dependent effective mass to be extracted from the experimental specific heat. Common to all these pictures is a rapid variation of the effective mass of a ^{3}He atom close to the Fermi surface.

The enhancement of the effective mass in the vicinity of the Fermi surface is, by itself, a well-known effect in nuclear physics.[7] The fact that this enhancement effect is substantially stronger in ^{3}He is usually attributed to the soft mode of spin-density fluctuations.

Microscopic studies of the effective-mass enhancement in nuclear matter have been performed on the basis of G-matrix[7] and variational[8,9] calculations. However, no attempts have yet been made to derive the energy (or momentum) dependence of the effective mass of liquid ^{3}He from the interatomic potential. In the present paper we show that the correlated-basis-function (CBF) approach provides a simple microscopic explanation and a semiquantitative determination of the effect.

The CBF theory[10] is presently the most powerful and efficient formalism which leads from a microscopic interaction to quantitative results for the properties of cold matter. It starts with a variational *ansatz* for the wave function which describes the average correlations between particles. State dependence is included through nonorthogonal perturbation theory. CBF allows a clean separation between state-dependent effects and the gross geometrical correlations induced by the core exclusion in a strongly interacting system. The inherent power of CBF was recognized about fifteen years ago by Feenberg and collaborators.[10,11] In the last decade enormous improvements in the variational theory have tended to overshadow the CBF theory. More recently, the growing awareness of the limitations in the purely variational approach has led to a fruitful union.

One attractive feature of the CBF-Jastrow approach is the close correspondence between its diagrams and those of ordinary perturbation theory. This means, however, that the "pedestrian" approach of calculating individual diagrams must rely heavily on a rapid convergence of the series. The strength of the CBF theory is the weakness of the effective interaction.

We present in this paper essentially the most complete evaluation of CBF-perturbation corrections which can be achieved with reasonable numerical effort in this pedestrian approach. For the ground-state energy we compute second-order corrections in the two- and three-body effective interaction and third-order corrections in the two-body effective interaction. In addition, we compute second- and third-order ring-diagram contributions to the (com-

plex) self-energy of a ^{3}He atom.

Our paper relies heavily on recent work on the ground-state energetics of helium and deuterium Fermion fluids.[12] The reader is urged to consult this paper for notational matters and a general outline of the optimized Fermi hypernetted-chain—CBF (FHNC-CBF) approach. In the next section we only outline the variational computation of the ground-state energy and its improvement by nonorthogonal perturbation theory. Explicit expressions are given for the second-order energy correction involving the two- and three-body effective interaction and the third-order term in the two-body interaction.

Section III discusses the single-particle excitation spectrum and its CBF corrections to the same order. Our numerical results for the Hartree-Fock dispersion 2 (HFDHE2) potential of Aziz *et al.*[13] are presented and discussed in Sec. IV. Two appendixes discuss the Monte Carlo integration of the $3p$-$3h$ diagrams and our approximations for the CBF effective interactions.

II. CBF COMPUTATION OF GROUND-STATE PROPERTIES

We deal with a Jastrow-correlated wave function

$$|\psi_0\rangle = F|\phi_0\rangle / \langle\phi_0|F^\dagger F|\phi_0\rangle^{1/2}, \quad F = \prod_{i<j} f(r_{ij}) , \tag{2.1}$$

where $|\phi_0\rangle$ is the usual ideal-gas Slater determinant. To choose the $f(r)$, we follow the "optimized FHNC" route described in detail in Ref. 12. In short, one solves the variational problem

$$0 = \left[\frac{\delta H_{00}}{\delta \ln f(r)} \right] \tag{2.2}$$

in a suitable approximation for the variational energy expectation value

$$H_{00} = \langle\psi_0|H|\psi_0\rangle . \tag{2.3}$$

[With a "suitable" approximation we mean one which preserves properties of the exact variational problem[14] as far as they are important for the determination of the optimum Jastrow function $f(r)$.] In practice, the four nonlinear FHNC equations[15] are extended by a set of linear equations (the so-called FHNC′ equations) which are generated from the FHNC equations by linearization and use the interaction as the driving term.[12] A simplified Newton-Raphson algorithm[16] or a suitable adaptation[12] of the working formulas of the "paired-phonon analysis (PPA)" technique[10,17] allows iterative improvement of the Jastrow correlation function until convergence is reached.

The variational estimate (2.1) of the ground-state energy may be improved by using the correlation operator F to generate a correlated, nonorthogonal basis of the A-particle Hilbert space through

$$|\psi_m\rangle = I_{mm}^{-1/2} F|\phi_m\rangle, \quad I_{mm} = \langle\Phi_m|F^\dagger F|\phi_m\rangle . \tag{2.4}$$

Here, $\{|\phi_m\rangle\}$ is a basis of the corresponding system of A noninteracting particles; we use a plane-wave basis $\{|\phi_m\rangle\}$. For convenience, we let $|\phi_0\rangle$ denote the noninteracting ground state, let $|\phi_{ph}\rangle$ denote the $1p$-$1h$ excitation $a_p^\dagger a_h|\phi_0\rangle$, etc.

In the nonorthogonal basis (2.4) we calculate matrix elements of the Hamiltonian and the unit operator. Diagonal matrix elements of H define the variational single-particle spectrum. For a $1p$-$1h$ correlated state $|\phi_{ph}\rangle$, the diagonal element

$$\begin{aligned} H_{ph,ph} - H_{00} &= \langle\psi_{ph}|H|\psi_{ph}\rangle - \langle\psi_0|H|\psi_0\rangle \\ &= e(p) - e(h) + O(A^{-1}) \end{aligned} \tag{2.5}$$

is exactly the difference between the variational particle and hole energies. The single-particle spectrum $e(k)$ is divided into kinetic and potential terms as follows:

$$e(k) \equiv \hbar^2 k^2/2m + u(k) . \tag{2.6}$$

The variational self-energy $u(k)$ is the analog of the Hartree-Fock self-energy in ordinary perturbation theory. Similarly, we define off-diagonal matrix-elements $(m \neq n)$

$$\begin{aligned} H'_{mn} &= \langle\psi_m|H - H_{00}|\psi_n\rangle , \\ \text{and} \qquad & \\ N_{mn} &= \langle\psi_m|\psi_n\rangle , \end{aligned} \tag{2.7}$$

of the Hamiltonian and the unit operator.

In terms of the (off-) diagonal quantities (2.5)—(2.7) the first terms of the perturbation expansion for the ground-state energy in the correlated basis (2.4) read[11]

$$\begin{aligned} E = H_{00} &- \sum_m H'_{0m} \frac{1}{H_{mm} - H_{00}} H'_{m0} \\ &+ \sum_{mn} H'_{0m} \frac{1}{H_{mm} - H_{00}} H'_{mn} \frac{1}{H_{nn} - H_{00}} H'_{n0} . \end{aligned} \tag{2.8}$$

Explicit application of the perturbation expansion (2.8) requires the specification of the number d of orbitals in which the states $|\phi_m\rangle$ and $|\phi_n\rangle$ differ from each other and from the filled Fermi sea $|\phi_0\rangle$. We will be concerned only with the cases $d=2$ and 3. In this case, we can write H'_{mn} and N_{mn} in the form of plane-wave matrix elements of (nonlocal) two- and three-body operators. In the $2p$-$2h$ case,

$$\langle \psi_{p_1p_2h_1h_2} \mid \psi_0 \rangle = \langle p_1p_2 \mid \mathcal{N}(12) \mid h_1h_2 \rangle_a \ ,$$

and

$$\langle \psi_{p_1p_2h_1h_2} \mid H - H_{00} \mid \psi_0 \rangle = \langle p_1p_2 \mid \mathcal{V}(12) \mid h_1h_2 \rangle_a$$
$$= \langle p_1p_2 \mid \mathcal{W}(12) \mid h_1h_2 \rangle_a + \tfrac{1}{2}[e(p_1)+e(p_2)-e(h_1)-e(h_2)] \langle p_1p_2 \mid \mathcal{N}(12) \mid h_1h_2 \rangle_a \ . \tag{2.9}$$

In this decomposition, the non-Hermitian operator $\mathcal{V}$ is expressed in terms of the Hermitian operators $\mathcal{W}$ and $\mathcal{N}$. (The subscript a indicates antisymmetrization.) The effective two-body interaction in the pp and hh channels may also be constructed from these operators. Inspection of higher-order terms in the CBF perturbation expansion leads to the definition of a general energy-dependent two-body interaction

$$\langle ij \mid \mathcal{V}(12,E) \mid kl \rangle = \langle ij \mid \mathcal{W}(12) \mid kl \rangle + \{ \tfrac{1}{2}[\mp e(i) \mp e(j) \mp e(k) \mp e(l)] + E \} \langle ij \mid \mathcal{N}(12) \mid kl \rangle \ . \tag{2.10}$$

In Eq. (2.10) the positive sign is taken for particle states and the negative one for hole states. In a given Goldstone-type diagram of the CBF perturbation series, the external energy E is the sum of all particle energies *minus* the sum of all energies at the "same time." In other words, the effective two-body interaction "knows" about the energy carried by the background at the same time. In general, we will drop the energy variable when we refer to $E=0$. For the case $d=3$, we similarly have

$$\langle \psi_{p_1p_2p_3,h_1h_2h_3} \mid \psi \rangle = \langle p_1p_2p_3 \mid \mathcal{N}(123) \mid h_1h_2h_3 \rangle_a \tag{2.11}$$

and

$$\langle \psi_{p_1p_2p_3,h_1h_2h_3} \mid H - H_{00} \mid \psi_0 \rangle = \langle p_1p_2p_3 \mid \mathcal{V}(123) \mid h_1h_2h_3 \rangle_a$$
$$= \langle p_1p_2p_3 \mid \mathcal{W}(123) \mid h_1h_2h_3 \rangle_a + \tfrac{1}{2}[e(p_1)+e(p_2)+e(p_3)-e(h_1)-e(h_2)-e(h_3)]$$
$$\times \langle p_1p_2p_3 \mid \mathcal{N}(123) \mid h_1h_2h_3 \rangle_a \ . \tag{2.12}$$

The straightforward generalization of the effective three-body interaction to other selections of particle and hole labels is unnecessary for our purposes.

In the present calculation for the ground-state energy we included the second- and third-order diagrams. Thus, the total energy is expressed in the form

$$E = H_{00} + (\delta E)_2^{(2)} + (\delta E)_2^{(3)} + (\delta E)_3^{(2)} \ , \tag{2.13}$$

where H_{00} is the variational energy expectation value, and

$$(\delta E)_2^{(2)} = -\tfrac{1}{4} \sum_{\substack{p_1p_2 \\ h_1h_2}} \frac{|\langle p_1p_2 \mid \mathcal{V}(12) \mid h_1h_2 \rangle_a|^2}{e(p_1)+e(p_2)-e(h_1)-e(h_2)} \tag{2.14}$$

and

$$(\delta E)_2^{(3)} = -\tfrac{1}{36} \sum_{\substack{p_1p_2p_3 \\ h_1h_2h_3}} \frac{|\langle p_1p_2p_3 \mid \mathcal{V}(123) \mid h_1h_2h_3 \rangle_a|^2}{e(p_1)+e(p_2)+e(p_3)-e(h_1)-e(h_2)-e(h_3)} \ . \tag{2.15}$$

The third-order contribution consists of ring diagrams and particle-particle and hole-hole ladders,

$$(\delta E)_3^{(2)} = (\delta E)_{pp} + (\delta E)_{hh} + (\delta E)_{ph} \ , \tag{2.16}$$

with

$$(\delta E)_{pp} = \tfrac{1}{8} \sum_{\substack{p_1p_2p_3p_4 \\ h_1h_2}} \frac{\langle h_1h_2 \mid \mathcal{V} \mid p_1p_2 \rangle_a \langle p_1p_2 \mid \mathcal{V}(12,-e(h_1)-e(h_2)) \mid p_3p_4 \rangle_a \langle p_3p_4 \mid \mathcal{V} \mid h_1h_2 \rangle_a}{[e(p_1)+e(p_2)-e(h_1)-e(h_2)][e(p_3)+e(p_4)-e(h_1)-e(h_2)]} \ , \tag{2.17}$$

$$(\delta E)_{hh} = \tfrac{1}{8} \sum_{\substack{h_1h_2h_3h_4 \\ p_1p_2}} \frac{\langle p_1p_2 \mid \mathcal{V} \mid h_1h_2 \rangle_a \langle h_1h_2 \mid \mathcal{V}(12,e(p_1)+e(p_2)) \mid h_3h_4 \rangle_a \langle h_3h_4 \mid \mathcal{V} \mid p_1p_2 \rangle_a}{[e(p_1)+e(p_2)-e(h_1)-e(h_2)][e(p_1)+e(p_2)-e(h_3)-e(h_4)]} \ , \tag{2.18}$$

and

$$(\delta E)_{ph}=\sum_{\substack{h_1h_2h_3\\p_1p_2p_3}}\frac{\langle h_1h_2\,|\,\mathscr{V}\,|\,p_1p_2\rangle_a\langle p_1h_3\,|\,\mathscr{V}(12,e(p_2)-e(h_2))\,|\,h_1p_3\rangle_a\langle p_3p_2\,|\,\mathscr{V}\,|\,h_3h_2\rangle_a}{[e(p_1)+e(p_2)-e(h_1)-e(h_2)][e(p_2)+e(p_3)-e(h_2)-e(h_3)]}\ . \tag{2.19}$$

The third-order contributions are the only ones in which the energy dependence of the effective interaction appears explicitly.

III. SELF-ENERGY

The perturbative expansion for the on-shell value of the self-energy may be generated from the CBF perturbation series through the Landau prescription

$$\epsilon(k)=\frac{\delta E}{\delta n(k)}\ . \tag{3.1}$$

In leading order, i.e., for the variational-energy expectation value, we obtain the variational spectrum (2.5). The variation of the second-order CBF correction, Eq. (2.14), leads to an expression which is formally identical to the on-shell value of the second-order self-energy.[8]

The variational construction (3.1) of the self-energy generates *a priori* only its on-shell value, which is consistent with the definition of the "statistical single-particle energies"[18] and adequate for the specific heat. In view of recent discussions on the energy and momentum dependence of the self-energy[5] we wish to generalize the expressions of Ref. 8 to off-shell energies. Within the present framework this is most easily done "by inspection," i.e., by considering higher-order CBF diagrams which have the second-order self-energy insertions as subdiagrams. We find that the full self-energy $\Sigma(k,E)$ must be calculated with the effective interaction taken at the off-shell energy E. Adopting the notation of Ref. 7, where subscript PO denotes polarization, and subscript CO denotes correlation,

$$\Sigma(k,E)=u(k)+\Sigma_{\rm PO}(k,E)+\Sigma_{\rm CO}(k,E)\ , \tag{3.2}$$

where

$$\Sigma_{\rm CO}(k,E)=\tfrac{1}{2}\sum_{phh'}\frac{|\,\langle pk\,|\,\mathscr{W}(12)+\frac{1}{2}[e(p)-e(k)-e(h)-e(h')+2E]\mathscr{N}(12)\,|\,hh'\rangle_a\,|^2}{E+e(p)-e(h)-e(h')-i\delta} \tag{3.3}$$

and

$$\Sigma_{\rm PO}(k,E)=\tfrac{1}{2}\sum_{pp'h}\frac{|\,\langle pp'\,|\,\mathscr{W}(12)+\frac{1}{2}[e(p)+e(p')+e(k)-e(h)-2E]\mathscr{N}(12)\,|\,hk\rangle_a\,|^2}{E+e(h)-e(p)-e(p')-i\delta}\ . \tag{3.4}$$

The arguments presented here for the second-order contribution to the self-energy are readily extended to higher-order corrections. Owing to the formal similarity between the CBF expansion and conventional perturbation theory, we neither repeat our reasoning for higher-order diagrams nor display them explicitly. The situation becomes somewhat different if we consider fourth-order diagrams. There, one actually observes some cancellations between the energy dependence of the two-body interaction and reducible contributions to the four-body interaction. However, these cancellations affect only the terms linear in the energy and do not contribute to the structure around the Fermi surface.

Numerical application of the formalism necessitates further discussion. With the full energy- and momentum-dependent self-energy available, one might think of solving a Dyson equation for the single-particle energies,

$$\epsilon(k)=\hbar^2k^2/2m+\Sigma(k,\epsilon(k))\ . \tag{3.5}$$

This generates effectively higher-order contributions to one of the energies in the propagator. Such a procedure is inconsistent unless a fully renormalized propagator is used. For this reason we consider the on-shell definition of the effective mass

$$\hbar^2k/m^*(k)=\hbar^2k/m+(d/dk)\Sigma(k,e(k)) \tag{3.6}$$

(in contrast to the distinction between "k mass" and "e mass"[7]), the adequate one in our perturbative calculation of the self-energy.

IV. NUMERICAL APPLICATION AND DISCUSSION

We have performed variational calculations for the HFDHE2 potential[13]; Ref. 12 describes the op-

timization procedure and outlines the sampling procedure for the Monte Carlo integration used to compute the perturbation corrections. The $3p$-$3h$ term (2.15) involves the computation of an additional 15-dimensional integral; a discussion of the sampling algorithm may be found in Appendix A. For the effective three-body interaction we used a generalized convolution approximation, as described in Appendix B.

Table I presents our results for the ground-state—energy contributions from the variational-energy expectation value and the distinct perturbative corrections. This breakup essentially reflects the consequences of the Jastrow *ansatz* (2.1) for the wave function. The smallness of the third-order *pp* and *hh* ladder diagrams simply means that the short-ranged correlations are generated adequately by the Jastrow wave functions. The second- and third-order ring diagrams describe the influence of (spin-) density fluctuations, propagator corrections, and "backflow" correlations. We will demonstrate later that the spin-density fluctuations are the most important. Finally, the $3p$-$3h$ term reflects the influence of three-body correlations.

We believe that the three-body correlations are somewhat overestimated by the $3p$-$3h$ term. Some reduction of this term and the third-order diagrams is to be expected from the inclusion of "elementary" diagrams in the FHNC calculation of the effective interaction, essentially caused by a reduction of the normalization factors (B13) at very small momenta.[19] Since the inclusion of higher-order three-particle diagrams, either pedestrian-wise or achieved through CBF-Bethe-Faddeev calculations, seems to require a forbidding numerical effort, we feel that the inclusion of explicit three-body correlation factors in the variational calculation is called for. The inclusion of these correlations leads to an additional binding energy[20,21] of roughly 0.4 K at the experimental equilibrium density when backflow is also included. It should largely eliminate the $3p$-$3h$ term, justifying thereby the further approximations made below. The variational Monte Carlo energy at the equilibrium density with backflow and three-body correlations is -1.91 K.[20] At this same density the pure Jastrow FHNC/C energy (-0.71 K) is 0.37 K higher than the corresponding Monte Carlo result.[20] The discrepancy is due to the neglect or approximation of elementary diagrams in the FHNC/C scheme.

Some care in handling the summation of higher-order CBF diagrams is required by an impending instability of the Jastrow wave function (2.1) against spin-density fluctuations.[12,21] This instability is not cured by introducing local spin-dependent correlations,[22] and will eventually show up as a divergence of the sum of all CBF ring diagrams. The problem will disappear if (1) instead of using the bare effective interaction as the driving term of the ring-diagram summation, we would, at higher orders, use particle-hole irreducible combinations of CBF diagrams, or (2) we would improve upon the Jastrow form (2.1) of the correlation operator by including three-body[20] or momentum-dependent correlations.

We expect that neither of the suggested improvements would have significant effects at the level of our present calculation. The reason for this is that our effective two-body interaction should not be identified with the quasiparticle interaction, but rather with an approximation to the general vertex function which also contains "particle-hole reducible" terms. These and the energy dependence discussed above tend to overshadow the particle-hole irreducible term at all but very low momentum transfers. Moreover, the dominant contributions to our perturbative corrections come from regions of moderate momentum transfer, $k_F < q < 2k_F$.

It is a general feature of the Jastrow variational *ansatz* that the spin-polarized system turns out to have a *lower* energy than the normal system, as demonstrated, for example, by Lhuillier and Levesque.[23] While formally the methods employed

TABLE I. Ground-state energy per particle for ^{3}He interacting via the HFDHE2 potential. Column 2 shows the variational-energy expectation value and columns 3–7 show the perturbative corrections described in the text. Column 8 gives the total energy and column 9 gives the standard deviation of the Monte Carlo integration.

ρ (Å^{-3})	H_0 (K)	$(\delta E)_2^{(2)}$ (K)	$(\delta E)_2^{(3)}$ (K)	$(\delta E)_{ph}$ (K)	$(\delta E)_{pp}$ (K)	$(\delta E)_{hh}$ (K)	E (K)	σ (K)
0.0076	−0.85	−0.24	−0.07	0.03	0.02	0.01	−1.10	0.01
0.0112	−1.19	−0.40	−0.22	0.17	−0.01	−0.05	−1.70	0.02
0.0130	−1.19	−0.49	−0.41	0.27	−0.03	−0.08	−1.93	0.03
0.0142	−1.12	−0.56	−0.55	0.35	−0.05	−0.10	−2.03	0.03
0.0148	−1.05	−0.64	−0.70	0.40	−0.06	−0.12	−2.17	0.05
0.0166	−0.71	−0.81	−1.07	0.57	−0.08	−0.17	−2.27	0.06
0.0180	−0.33	−0.94	−1.53	0.73	−0.10	−0.22	−2.39	0.08

here are applicable, there is a problem. The optimal FHNC/C calculation gives a single-particle spectrum $u(k)$ which indicates that the uncorrelated ground state is not a suitable starting point for this calculation. The results of Ref. 23 indicate that perturbation corrections to the energy of the spin-polarized system are likely to be small, but we do not at present feel justified in calculating them with the methods used here.

Let us now turn to the discussion of our numerical results for the self-energy. In this calculation we have retained only the contributions due to the second- and third-order ring diagrams. The third-order ladder diagrams were omitted due to the smallness of their contribution to the energy. Those arising from the $3p$-$3h$ interaction would, in our conviction, be strongly overestimated by the omission of three-body correlation factors in F. We expect that the inclusion of a three-body correlation factor would essentially eliminate the $3p$-$3h$ contributions to the self-energy but will not modify the two-body effective interaction enough to noticeably alter the second- and third-order ring diagrams.

Figure 1 compares our CBF single-particle energies and the on-shell self-energy in second and third order with the "schematic model" calculation of Ref. 6. At and above k_F we find excellent agreement with the phenomenological fit of Ref. 6. It is also worth noting that our variational single-particle energies are in good agreement with those of Ref. 6,

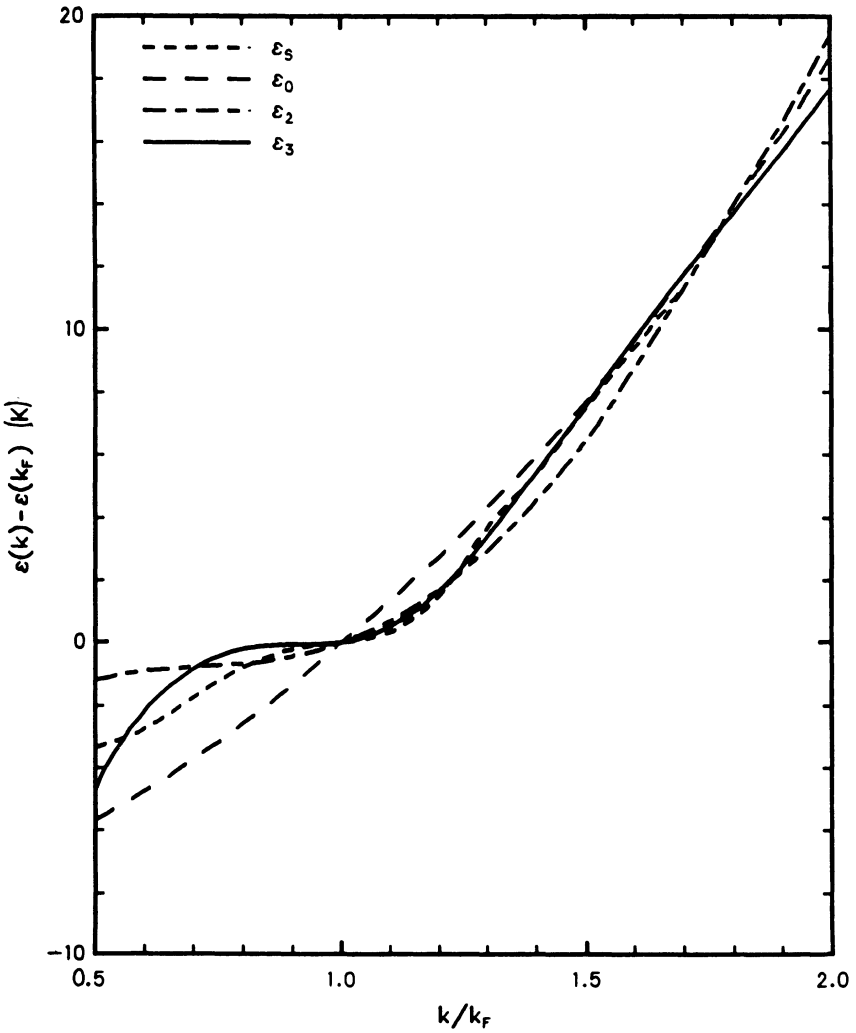

FIG. 1. Real part of the single-particle spectrum $\epsilon(k)=\hbar^2k^2/2m+\Sigma(k,e(k))$ at $\rho=0.0166$ Å^{-3} is given as a function of momentum k/k_F. Solid and long-short dashed lines display our third- and second-order CBF results. The long-dashed curve displays the variational spectrum $e(k)$, whereas the short-dashed curve represents the self-energy fitted to the specific heat (Ref. 6).

which include explicit backflow correlations. At this juncture we stress that the effective mass obtained from the variational spectrum must not be confused with the so-called "k mass," which also obtains substantial corrections from the higher-order self-energy diagrams.

Figure 2 shows the imaginary part of the self-energy coming from second- and third-order ring diagrams. While this is not experimentally accessible, the size of the imaginary part determines the quasiparticle lifetime and hence the range of validity of the quasiparticle model. The convergence appears good in the vicinity of the Fermi surface, $0.75k_F < k < 1.5k_F$. At higher momenta, the second energy denominator in the third-order ring diagram generates a secondary minimum. One can expect this minimum to be filled out somewhat by higher-order ring-diagram contributions, but it indicates a flattening of the imaginary part at higher momenta. We should also note that the real part of the self-energy cannot be obtained from the imaginary part using a Kramers-Kronig relation: Upon canceling all energy numerator terms occurring in the effective interaction against energy denominators, one is left with a remainder which does not have an energy denominator at all. This term is real and of the same diagrammatical structure as the variational single-particle energies.

Figure 3 shows the effective mass obtained from the on-shell differentiation of the second- and third-order self-energy as a function of momentum. To consider m^* as a function of energy, the momentum k must be related to an energy using the spectrum of Fig. 1. It becomes clear that a kink in the

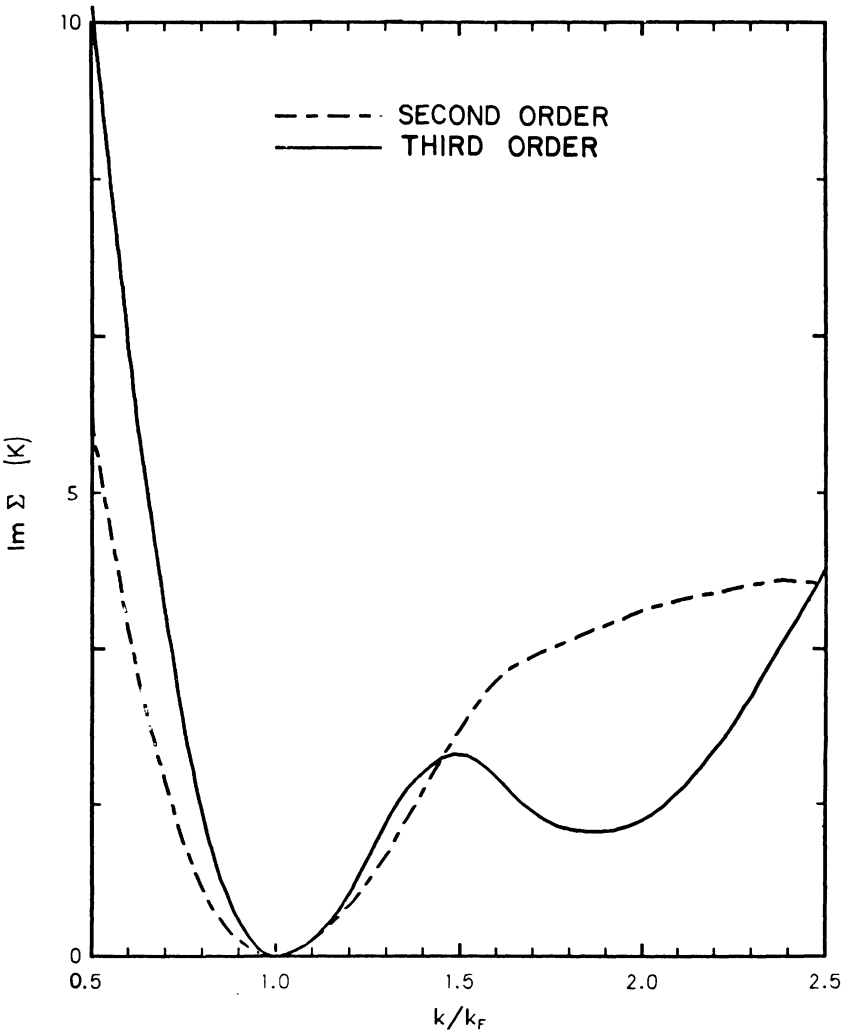

FIG. 2. Imaginary part of the self-energy in second- and third-order CBF's is given as a function of momentum. Conventions are the same as in Fig. 1.

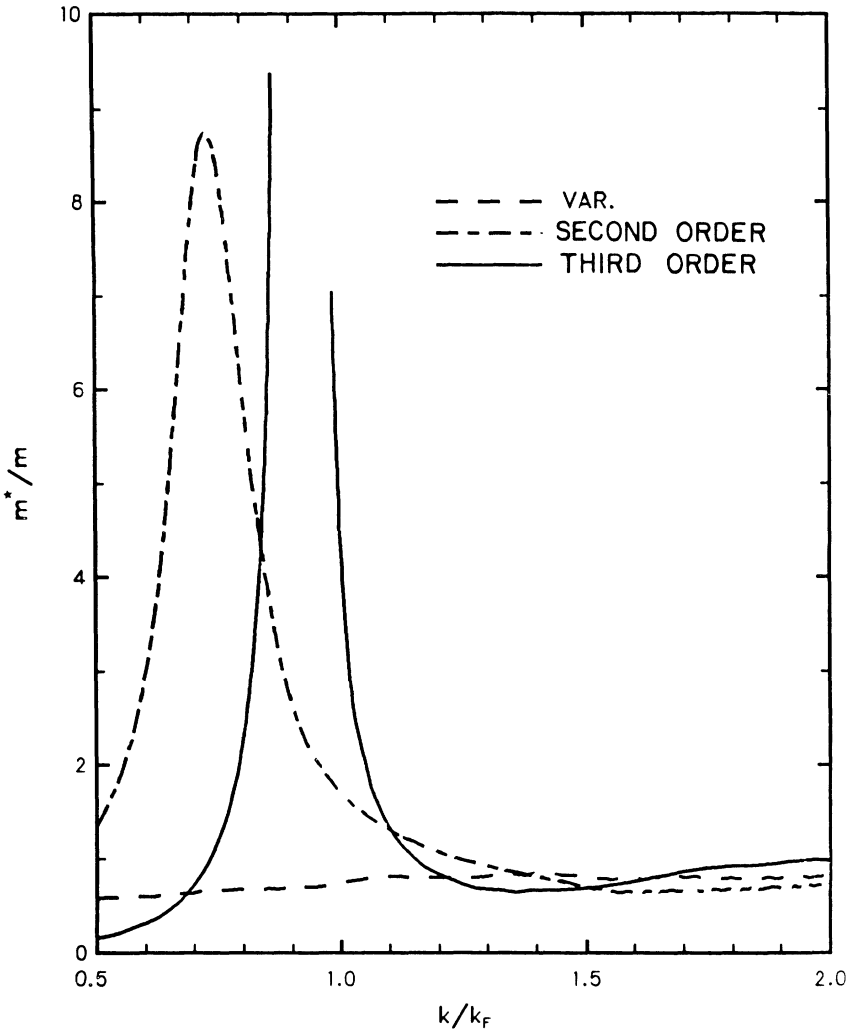

FIG. 3. Effective mass obtained from the variational single-particle energies and in second- and third-order CBF's is plotted as a function of momentum (lower scale). See Fig. 1 for further explanations.

spectrum around the Fermi surface substantially compresses the enhancement peak of the effective mass when m^* is considered as a function of energy instead of momentum. In other words, a large effective mass, even if it extends over a *momentum region* comparable to k_F, is always transformed into a narrow enhancement peak as a function of *energy*.

Compared with recent experimental data,[24] our effective mass looks somewhat like the one obtained experimentally at higher pressures. To some extent this may be attributed to the fact that our model is in a sense a "high-pressure" calculation. Note that the experimental equilibrium density $\rho_0 \approx 0.0166$ Å^{-3} at which our calculation was performed is above the variationally calculated equilibrium density $\rho_0^{\text{var}} \approx 0.013$ Å^{-3}. Some computed effective-mass-ratio approximations at the Fermi surface range from about 2 to 16 as the density increases from 0.011 to 0.020 Å^{-3}. It is difficult to know how to assign pressures to these for comparison with Ref. 24. Our values of the effective mass at k_F are also affected by the continuing steep rise before k_F, which makes a quantitative, purely microscopic determination very difficult.

In order to trace the source of the large effective mass and its rapid variation, we have computed separately the polarization diagram $\Sigma_{\text{PO}}(k,e(k))$ in the density and in the spin-density channels (Fig. 4). We find that the corrections to the spectrum come almost entirely from the spin-density channel. This had to be expected since density fluctuations are already included in the FHNC calculation of the CBF spectrum; the perturbation corrections reflect essentially propagator modifications.

The rapid variation of the spectrum is found to be mainly due to the drop of the correlation-diagram

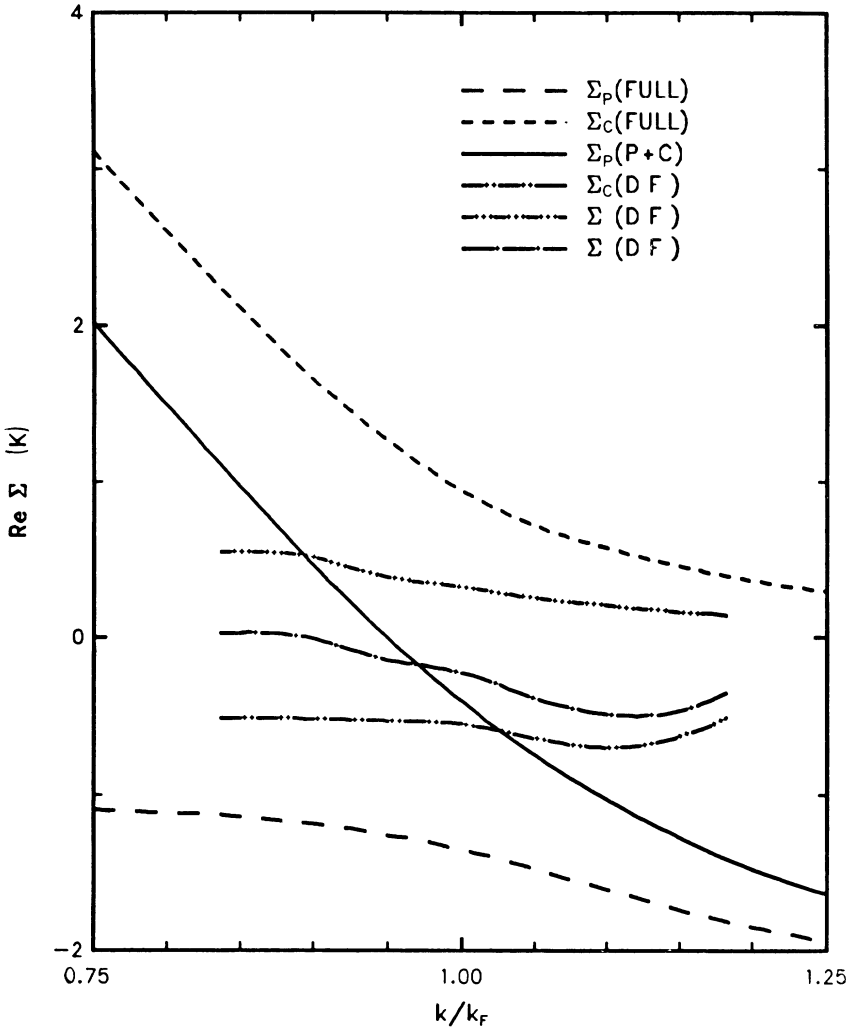

FIG. 4. Full polarization and correlation diagrams and the contributions, labeled by DF due to density fluctuations are shown near k_F. Sum of the polarization and correlation diagrams are labeled by $\Sigma(P+C)$ and Σ(DF).

equation (3.3) at and above k_F. The effect may be understood as the concerted action of phase-space effects and the finite range of the effective interaction: As the momentum of the incoming particle increases, the interaction has to carry more and more momentum. The decrease of the interaction with growing momentum transfer, together with the growing energy denominator, acts to suppress entirely the correlation diagram within $0.5k_F$.

Assuming the single-particle spectrum to be independent of the temperature, we may calculate the specific heat per particle $C_v(T)$ with the relation

$$C_v(T)=\frac{3}{k_F^3}\int_0^\infty \frac{dk\,k^2x^2\exp(x)}{[1+\exp(x)]^2}\,,$$
$$x=[\epsilon(k)-\epsilon(k_F)]/(k_BT)\,. \quad (4.1)$$

The results of this computation for the variational, second-order, and third-order ring diagrams are shown in Fig. 5, along with the "experimental" curve from Ref. 6. It almost went without saying that the low-temperature specific heat is extremely sensitive to minute changes in the slope of the single-particle spectrum when that slope is nearly zero. That slope has changed very little (Fig. 1) in going from second to third order, but results in an appreciable change in the low-temperature specific heat. The third-order corrections do seem to improve the behavior of the specific heat at higher temperatures.

Let us finally turn to the question of the energy and momentum dependence of the effective mass. Experience from studies of the self-energy in nuclear matter[7] have led to the conclusion that the variation of the effective mass is essentially due to the energy dependence. Since ^{3}He is a completely different physical system, one has to be careful in carrying over such an assumption.

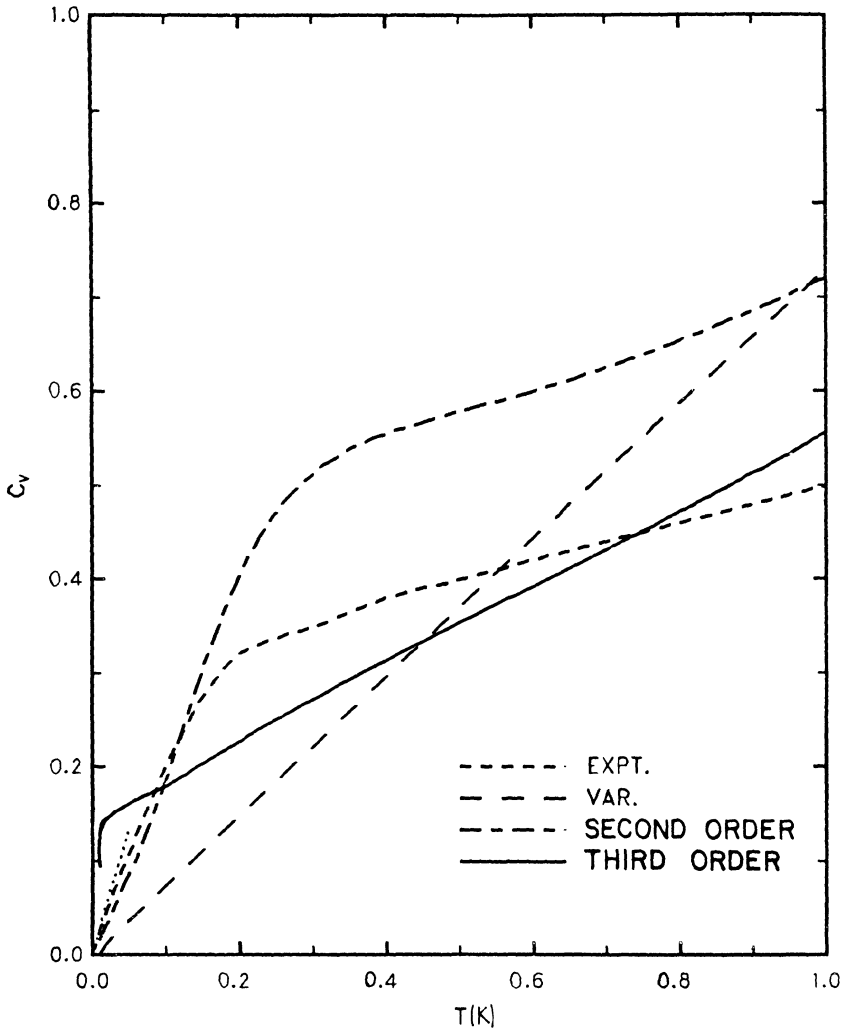

FIG. 5. Specific heat obtained from the variational and the second- and third-order CBF spectrum are compared with experiment. Dotted line shows the results of Ref. 24. See Fig. 1 for further descriptions.

To study the energy and momentum dependence individually, we have computed the off-shell self-energy in the second-order CBF approximation. A contour plot is shown in Fig. 6. We find that energy and momentum variation of $\Sigma(k,E)$ are comparable. From this it should be clear that our model cannot give justification for the assumption that one of the two dependencies is dominant.

Note added in proof. After this work had been finished, it was recognized that the coupling to the zero-sound mode generates a secondary enhancement of the effective mass above $k \approx 2k_F$. This effect, which comes from summing all CBF ring diagrams, is not included in the present work. By keeping the full nonlocality of the exchange term, the calculation presented here provides a more accurate determination of the self-energy near the Fermi surface.

ACKNOWLEDGMENTS

We would like to thank the nuclear theory group in Stony Brook for hospitality when the work was begun. Stimulating discussions with K. Bedell, G. E. Brown, J. W. Clark, S. Fantoni, B. L. Friman, A. D. Jackson, V. R. Pandharipande, C. J. Pethick, D. P. Pines, D. G. Sandler, and P. J. Siemens are gratefully acknowledged. We thank D. S. Greywall and P. A. Busch for communicating their results to us prior to publication. The work was supported in part by the National Science Foundation (NSF) under Grant No. PHY 78-26582 and PHY 82-06325, the U.S. Department of Energy under Contract No. DE-AC02-76ER13001, and the Deutsche Forschungsemeinschaft through a Heisenberg Fellowship (E.K.).

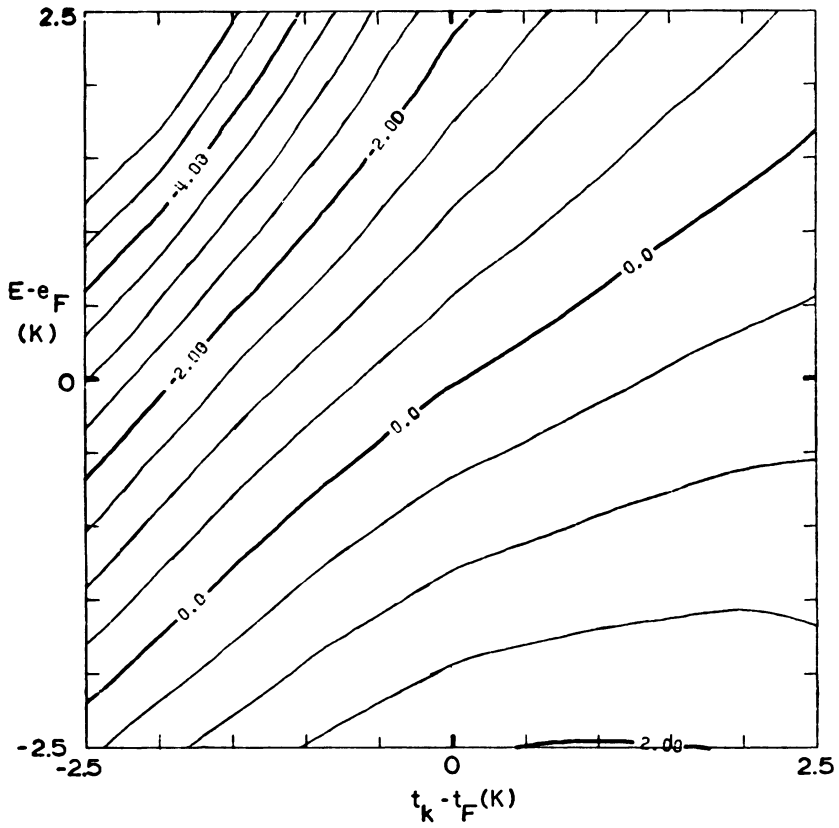

FIG. 6. Contours of the real part of $\Sigma(k,E)$ in second-order CBF are shown as a function of energy and momentum. Momentum k is expressed in terms of its associated kinetic energy $t(k)=\hbar^2k^2/2m$.

APPENDIX A: THE 3p-3h MONTE CARLO INTEGRATION

The desired integral (2.15) requires integration over three-particle and three-hole momenta with an overall momentum-conserving δ function. Letting $\vec{q}_i=\vec{p}_i-\vec{h}_i$, the integral becomes

$$(E)_2^{(3)}=-\frac{1}{36}\int\frac{d^3q_1}{(2\pi)^3}\frac{d^3q_2}{(2\pi)^3}\frac{d^3q_3}{(2\pi)^3}\delta(\vec{q}_1+\vec{q}_2+\vec{q}_3)\prod_{i=1}^{3}\int\frac{d^3\vec{h}_i}{(2\pi)^3}\theta(k_F-h_i)\theta(|\vec{h}_i+\vec{q}_i|-k_F)\left[\frac{|\langle\cdots\rangle_a|^2}{E}\right]. \tag{A1}$$

The q_i are first drawn from a density

$$\rho(\vec{q}_1,\vec{q}_2,\vec{q}_3)=Q(q_1)Q(q_2)Q(|\vec{q}_1+\vec{q}_2|)\delta(\vec{q}_1+\vec{q}_2+\vec{q}_3)\,. \tag{A2}$$

This may be done most easily by considering

$$\int d^3q_1d^3q_2d^3q_3\rho(\vec{q}_1,\vec{q}_2,\vec{q}_3)\equiv 8\pi^2\int_0^\infty q_1Q(q_1)dq_1\int_0^\infty q_2Q(q_2)dq_2\int_{|q_1-q_2|}^{q_1+q_2}tQ(t)dt\,. \tag{A3}$$

First choose q_1 with relative weight

$$p(q_1)\propto q_1Q(q_1)[Q^*Q](q_1)\,, \tag{A4}$$

and direct it in the $\hat{z}$ direction. The "$*$" denotes a convolution. Given q_1, then choose q_2 with the relative weight

$$p(q_2\,|\,q_1)\propto q_2Q(q_2)\int_{|q_1-q_2|}^{|q_1+q_2|}tQ(t)dt\,. \tag{A5}$$

Next choose $t=|\vec{q}_1+\vec{q}_2|$ with weight

$$p(t\,|\,q_1,q_2)\propto tQ(t)\,. \tag{A6}$$

The proportionality factor in (A5) depends on q_1, while the factor in (A6) depends on both q_1 and q_2. Letting $\vec{t}=\vec{q}_1+\vec{q}_2$, we have

$$t^2=q_1^2+q_2^2+2\vec{q}_1\cdot\vec{q}_2\,,$$

which may be solved for the angle between $\hat{q}_1,\hat{q}_2$. The azimuthal component of $\hat{q}_2$ is arbitrary. Finally, $\vec{q}_3=-(\vec{q}_1+\vec{q}_2)$. Then the h_i are drawn independently from the distributions

$$\Theta(k_F-h_i)\Theta(|\vec{h}_i+\vec{q}_i|-k_F)$$

according to the algorithm of Ref. 12. The matrix elements and energy denominators may then be calculated. The function Q is chosen empirically to accelerate convergence.

APPENDIX B: EFFECTIVE TWO- AND THREE-BODY INTERACTIONS

The basic building blocks for the effective two- and three-body overlap and Hamiltonian matrix elements are provided by the optimized FHNC/C calculation of the variational energy. The reader is referred to Refs. 12 and 15 for the definition of the relevant quantities; as usual we denote the three-dimensional Fourier transform with a tilde. The raw material $(\Gamma_{dd},\Gamma'_{dd},\tilde{X}_{cc},u)$ obtained from an (optimized) FHNC calculation must be combined to generate the required matrix elements of $\mathcal{N}(12)$, $\mathcal{N}(123)$, $\mathcal{W}(12)$, and $\mathcal{W}(123)$. We start with the two-body operator $\mathcal{N}(12)$. This has the structure[12]

$$\langle ij|\mathcal{N}(12)|kl\rangle=D_2^{-1}\langle ij|\mathcal{N}^B(12)|kl\rangle\ , \tag{B1}$$

with D_2 given by

$$D_2=\{[1-\tilde{X}_{cc}(p_i)][1-\tilde{X}_{cc}(p_j)]\times[1-\tilde{X}_{cc}(p_k)][1-\tilde{X}_{cc}(p_l)]\}^{1/2}\ . \tag{B2}$$

Here, and further below, we denote with p_i the momentum carried by the plane-wave orbital i. The simplest local approximation to $\mathcal{N}^B(12)$ is the FHNC quantity $\Gamma_{dd}(r_{12})$. However, in order to assure the correct Landau limit $|\vec{p}_i-\vec{p}_k|\to 0$, we have to include additional "elementary" diagrams[12]:

$$\langle ij|\mathcal{N}^B(12)|kl\rangle=[1+E_{ecc}(i,k)]\langle ij|\Gamma_{dd}(r)|kl\rangle\times[1+E_{ecc}(j,l)]\ . \tag{B3}$$

These elementary diagrams are approximated by a polynomial fit, in the region $0<|\vec{p}_i-\vec{p}_k|<2k_F$ where they are nonzero, which is determined by their values at the boundaries,

$$E_{ecc}(i,k)=\tfrac{1}{2}[S_F(|\vec{p}_i-\vec{p}_k|)-1]\times[X_{cc}(p_i)+X_{cc}(p_k)]\ . \tag{B4}$$

Here $S_F(k)$ is the static structure function of a noninteracting Fermi gas. Note that the elementary diagrams cancel the normalization factor D_2 in the Landau limit. The inclusion of these diagrams is important since the long range of the optimal correlation functions would otherwise lead to divergences.

The calculation of the spectrum

$$e(k)=\hbar^2k^2/2m+u(k) \tag{B5}$$

requires the solution of an additional set of linear equations, the so-called FHNC′ equations. These are implicit in the optimization procedure. Similar to (B1), $\mathcal{W}(12)$ may be written as

$$\langle ij|\mathcal{W}(12)|kl\rangle=D_2^{-1}\{\langle ij|\mathcal{W}^B(12)|kl\rangle+\tfrac{1}{2}[u(p_i)+u(p_j)+u(p_k)+u(p_l)]\langle ij|\mathcal{N}^B(12)|kl\rangle\}\ . \tag{B6}$$

The dominant term of $\mathcal{W}^B(12)$ is, again, a local function,

$$\mathcal{W}_{\rm loc}(12)=\Gamma'_{dd}(r)+(\hbar^2\nabla^2/4m)\Gamma_{dd}(r)\ , \tag{B7}$$

but to ensure the correct Landau limit, we have to include elementary and kinetic-energy diagrams,

$$\begin{aligned}D_2\langle ij|\mathcal{W}(12)|kl\rangle=&[1+E_{ecc}(i,k)][1+E_{ecc}(j,l)]\langle ij|\mathcal{W}_{\rm loc}(12)|kl\rangle\\&+\{[1+E_{ecc}(i,k)][U'_{ecc}(j,l)+T_{ecc}(j,l)]\\&+[1+E_{ecc}(j,l)][U'_{ecc}(i,k)+T_{ecc}(i,k)]\}\langle ij|\Gamma_{dd}(12)|kl\rangle\ ,\end{aligned} \tag{B8}$$

with

$$T_{ecc}(i,k)=(\hbar^2/4m)\{-(\vec{p}_i-\vec{p}_k)\cdot[\vec{p}_iY(p_i)-\vec{p}_kY(p_k)]+\vec{p}_i\cdot\vec{p}_kY(p_i)Y(p_k)\} \tag{B9}$$

and $U'_{ecc}(i,k)$ being a combination of separable and elementary contributions

$$2U'_{ecc}(i,k)=[u(p_i)+u(p_k)][1+E_{ecc}(i,k)]+2E'_{ecc}(i,k)\ , \tag{B10}$$

which is approximated as

$$2U'_{ecc}(i,k)=S_F(|\vec{p}_i-\vec{p}_k|)[u(p_i)+u(p_k)]\ . \tag{B11}$$

Again, the approximation (B11) originates from studies of the exact properties of $E'_{ecc}(i,k)$ for large momenta

and in the Landau limit. Note that the separable (second) term in Eq. (B6) is included in $U'_{ecc}(i,k)$. The function $Y(p)$ is defined in Ref. 12.

Extending the analysis of Ref. 12 to the three-body operators, we are led to a decomposition of $\mathcal{N}(123)$ in the form

$$\langle ijk \,|\, \mathcal{N}(123) \,|\, lmn \rangle = D_3^{-1} \langle ij \,|\, \mathcal{N}^B(123) \,|\, lmn \rangle \ , \tag{B12}$$

where

$$D_3 = \{[1-\tilde{X}_{cc}(p_i)][1-\tilde{X}_{cc}(p_j)][1-\tilde{X}_{cc}(p_k)][1-\tilde{X}_{cc}(p_l)][1-\tilde{X}_{cc}(p_m)][1-\tilde{X}_{cc}(p_n)]\}^{1/2} \ , \tag{B13}$$

and the local portion of $\mathcal{N}^B(123)$ is the connected part of the three-body distribution function $\Gamma_{ddd}(\vec{r}_1,\vec{r}_2,\vec{r}_3)$. In order to guarantee the correct Landau limit we must again include the factorizable elementary diagrams [Eq. (B3)],

$$\langle ijk \,|\, \mathcal{N}^B(123) \,|\, lmn \rangle = [1+E_{ecc}(i,l)][1+E_{ecc}(j,m)][1+E_{ecc}(k,n)] \langle ijk \,|\, \Gamma_{ddd}(\vec{r}_1,\vec{r}_2,\vec{r}_3) \,|\, lmn \rangle \ . \tag{B14}$$

In the actual calculation, we have used a generalized convolution approximation[10] for $\Gamma_{ddd}(\vec{r}_1,\vec{r}_2,\vec{r}_3)$,

$$\Gamma_{ddd}(\vec{r}_1,\vec{r}_2,\vec{r}_3) = [\Gamma_{dd}(r_{12})\Gamma_{dd}(r_{13}) + \text{c.p.} + \rho \int d^3r_4 \Gamma_{d\bullet}(r_{14})\Gamma_{d\bullet}(r_{24})\Gamma_{d\bullet}(r_{34}) \ , \tag{B15}$$

with

$$\tilde{\Gamma}_{d\bullet}(k) = \tilde{\Gamma}_{dd}(k) S_F(k) \tag{B16}$$

and c.p. a cyclic permutation. The modification of the last term by the factor $S_F(k)$ takes the exchange effects at the internal point r_4 approximately into account. Owing to the long range of the correlations this inclusion of exchange terms is necessary to guarantee the finiteness of the matrix elements.

Finally, the three-body term $\langle ijk \,|\, \mathcal{W}(123) \,|\, lmn \rangle$ has the form

$$\begin{aligned} \langle ijk \,|\, \mathcal{W}(123) \,|\, lmn \rangle = D_3^{-1} \{ & \langle ijk \,|\, \mathcal{W}^B(123) \,|\, lmn \rangle \\ & + \tfrac{1}{2}[u(p_i)+u(p_j)+u(p_k)+u(p_l)+u(p_m)+u(p_n)] \langle ijk \,|\, \mathcal{N}^B(123) \,|\, lmn \rangle \} \ , \end{aligned} \tag{B17}$$

with the "local" terms

$$\begin{aligned} \langle ijk \,|\, \mathcal{W}^B_{\text{loc}}(123) \,|\, lmn \rangle = & \langle ijk \,|\, \Gamma'_{ddd}(123) \,|\, lmn \rangle \\ & - (\hbar^2/8m)[(\vec{p}_i-\vec{p}_l)^2+(\vec{p}_j-\vec{p}_m)^2+(\vec{p}_k-\vec{p}_n)^2] \langle ijk \,|\, \Gamma_{ddd}(123) \,|\, lmn \rangle \ . \end{aligned} \tag{B18}$$

The three-body term $\Gamma'_{ddd}(123)$ is defined diagrammatically by the prescription that each bond $\Gamma_{dd}(r)$ in $\Gamma_{ddd}(123)$ has to be replaced, in turn, by a function $\Gamma'_{dd}(r)$. This also defines our convolution approximation for Γ'_{ddd}. Including the necessary elementary diagrams, the final representation of the three-body operator $\mathcal{W}(123)$ is

$$\begin{aligned} D_3 \langle ijk \,|\, \mathcal{W}(123) \,|\, lmn \rangle = & [1+E_{ecc}(i,l)][1+E_{ecc}(j,m)][1+E_{ecc}(k,n)] \langle ijk \,|\, \mathcal{W}^B_{\text{loc}}(123) \,|\, lmn \rangle \\ & + \{[1+E_{ecc}(i,l)][1+E_{ecc}(j,m)][U'_{ecc}(k,n)+T'_{ecc}(k,n)] + \text{c.p.}\} \langle ijk \,|\, \Gamma_{ddd}(123) \,|\, lmn \rangle . \end{aligned} \tag{B19}$$

In order to confirm the adequacy of the convolution approximation we mention that the third-order term of the convolution approximation contributes at the highest density an energy of the order of 0.1 K.

---

*Present address: Institute for Theoretical Physics, University of California Santa Barbara, Santa Barbara, CA 93106.

[1] J. Wilks, *The Properties of Liquid and Solid Helium* (Clarendon, Oxford, England, 1967).

[2] J. C. Wheatley, Rev. Mod. Phys. 47, 415 (1975).

[3] T. A. Alvesalo, T. Haavasoja, P. C. Main, M. T. Manninen, J. Ray, and L. M. M. Rehn, Phys. Rev. Lett. 43, 1509 (1979); T. A. Alvesalo, T. Haavasoja, M. T. Manninen, and A. T. Sointe, *ibid.* 44, 1076 (1980).

[4] P. R. Roach, M. W. Meisel, and Y. Eckstein, Phys. Rev. Lett. 48, 330 (1982).

[5]G. E. Brown, C. J. Pethick, and A. Zaringhalam, J. Low Temp. Phys. 48, 349 (1982).
[6]S. Fantoni, V. R. Pandharipande, and K. E. Schmidt, Phys. Rev. Lett. 48, 878 (1982).
[7]V. Bernard and C. Mahaux, Phys. Rev. C 23, 888 (1981); J. P. Jeukenne, A. Lejeune, and C. Mahaux, Phys. Rep. 25C, 83 (1976).
[8]E. Krotscheck, R. A. Smith, and A. D. Jackson, Phys. Lett. 104B, 421 (1981).
[9]S. Fantoni, B. Friman, and V. R. Pandharipande (unpublished).
[10]E. Feenberg, *Theory of Quantum Fluids* (Academic, New York, 1969).
[11]J. W. Clark and E. Feenberg, Phys. Rev. 113, 388 (1959); C.-W. Woo, Phys. Rev. 151, 138 (1966); H.-T. Tan and E. Feenberg, *ibid.* 176, 370 (1968); E. Feenberg and C.-W. Woo, *ibid.* 137, A391 (1965).
[12]E. Krotscheck, R. A. Smith, J. W. Clark, and R. M. Panoff, Phys. Rev. B 24, 6383 (1981).
[13]R. A. Aziz, V. P. S. Nain, J. S. Carley, W. L. Taylor, and G. T. McConville, J. Chem. Phys. 70, 4330 (1979).
[14]E. Krotscheck, Phys. Rev. A 15, 397 (1977); E. Krotscheck and W. Kundt, Phys. Lett. 71B, 19 (1977).
[15]J. W. Clark, in *Progress in Nuclear and Particle Physics,* edited by H. Wilkinson (Pergamon, Oxford, England, 1979), Vol. 2.
[16]J. C. Owen, Phys. Lett. 89B, 303 (1980); Phys. Rev. B 23, 2169 (1981).
[17]C. C. Chang and C. E. Campbell, Phys. Rev. B 15, 4238 (1977).
[18]C. J. Pethick and G. M. Carneiro, Phys. Rev. A 7, 304 (1973); G. M. Carneiro and C. J. Pethick, Phys. Rev. B 16, 1933 (1977).
[19]S. Fantoni and Q. Usmani, private communication.
[20]K. E. Schmidt, M. A. Lee, M. H. Kalos, and G. V. Chester, Phys. Rev. Lett. 47, 807 (1981).
[21]D. Levesque, Phys. Rev. B 21, 5159 (1980).
[22]C. E. Campbell and K. E. Kürten, J. Low Temp. Phys. 44, 149 (1981); J. C. Owen and G. Ripka, Phys. Rev. B 25, 4914 (1982).
[23]C. Lhuillier and D. Levesque, Phys. Rev. B 23, 2203 (1981).
[24]D. S. Greywall and P. A. Busch, Phys. Rev. Lett. 49, 146 (1982).
[25]B. L. Friman and E. Krutscheck, Phys. Rev. Lett. 49, 1705 (1982).